Investigation of thermal breakage and heat transfer in single, insulated and laminated glazing under fire conditions

Yu Wang[b], Qingsong Wang[a,c*], Jennifer X. Wen[d], Jinhua Sun[a], K.M. Liew[e]

[a]*State Key Laboratory of Fire Science, University of Science and Technology of China, Hefei 230026, P.R. China*

[b]*Department of Civil & Environmental Engineering, National University of Singapore, Singapore 117576, Singapore*

[c]*Collaborative Innovation Center for Urban Public Safety, Anhui Province, Hefei 230026, P.R. China*

[d]*Warwick FIRE, School of Engineering, University of Warwick, Coventry CV4 7AL, UK*

[e]*Department of Architecture and Civil Engineering, City University of Hong Kong, Tat Chee Avenue, Kowloon, Hong Kong*

Abstract

To make constructions more artistic, various new kinds of glazing are increasingly employed in building envelopes. However, when subjected to a fire, these glass façades may easily break and fall out, significantly accelerating the development of enclosure fire. Thus, it is necessary to investigate and compare their different fire performance and breakage mechanisms. In this work, a total of ten tests, including single coated, insulated and laminated glazing, were heated by a 500×500 mm^2 pool fire. Breakage time, glass surface and air temperature, incident heat flux and crack initiation and propagation were obtained. The critical conditions of three different kinds of glazing were determined. It was established that the insulated and laminated glass can survive longer than the single

[*]Corresponding author: Tel.: +86-551-6360-6455; fax: +86-551-6360-1669. *E-mail:* pinew@ustc.edu.cn (Q.S. Wang)
First author: E-mail: ywang232@mail.ustc.edu.cn (Y. Wang)

glass. The thermal resistance from the air gap and fire side glass pane was found to play a key role for the ambient side pane of the insulated glazing. Although both panes of the laminated glazing broke, it could be held together by the layer of gel, effectively avoiding the formation of a new vent. Numerical simulations were performed to investigate the heat transfer process through the glazing panels and the temperatures in the glazing were predicted well. Suggestions for glass fire resistance design are proposed.

Keywords: glass thermal breakage; heat transfer; finite element method; single glazing; double glazing

Nomenclature Listing

A	glass area (m^2)	δ	glass thickness (m)
c	specific heat (J/(kg·K))	ε	emissivity
h	convection heat transfer coefficient (W/(m^2·K))	E	modulus of elasticity (Pa)
R	thermal resistance (m^2·K/W)	ν	poisson's ratio
k	thermal conductivity (W/(m·K))	ρ	density (kg/m^3)
L	length (m)	σ	Stefan-Boltzmann constant
m	mass (kg)	**subscripts**	
q	heat flux (kW/m^2)	1-9	thermocouple number
T	temperature (K)	∞	air
t	time (s)	c	contact
x	dimension into glass (mm)	g	generation; Bulk glass
y	away lower edge (mm)	gel	gel layer
z	along left edge (mm)	in	incident
Greek		R	reference
β	thermal expansion coefficient (1/K)	S	surface
Δ	difference	*sur*	surrounding

1. Introduction

In recent years, the trends in the design of glass facades have radically changed with more frequent use of different kinds of glazing. This is the result of an architectural movement where aesthetic considerations play a relevant role [1]. Therefore, instead of clear single glazing, coated, insulated and laminated glasses, due to their energy conservation, good appearance and better illumination, are being increasingly used in high-rise building envelopes in China [2-4], as well as some other parts of the world [5, 6]. However, unlike concrete and steel, glass is a brittle material that may easily break under extreme conditions [7, 8]. When subjected to a fire, the breakage and fallout of glass create a new vent for fresh air to enter and for the fire to spread outside. In high-rise buildings, the creation of such vents will rapidly accelerate the spreading of fire to different floors and also create torch effects. The extensive use of different types of glazing inevitably brings more potential fire risk and make it difficult for building structures to comply with national fire codes.

In the 1st IAFSS Symposium, Emmons highlighted the importance of glass breakage to building structure integrity [9]. Subsequently, a large number of experimental, theoretical and numerical investigations have been conducted to investigate the breakage mechanism of glazing in fire [10]. Keski-Rahkonen theoretically determined the critical temperature difference between the fire exposed and covered areas [11, 12]. Shields et al. heated the glass panes in an ISO room with a pool fire placed in the center and corner of the compartment [13, 14]. Based on 59 tests, Joshi and Pagni [15, 16] used a Weibull distribution to analyze the probability of glass breakage. Harada et al. [17] conducted 50 radiant heating tests of float and wired glass with varying incident heat flux (3-9 kW/m^2) in conditions with or without lateral restraint. In addition, models of various complexity

have been developed to predict the time to first crack, such as BREAK1 [18] and EASY [19]. From these studies, a consensus has been reached that the primary reason for glass breakage is the excessive thermal stress resulting from the temperature difference between the exposed and covered areas.

Nevertheless, compared to the work on single clear glazing, studies concerning other types of glass are relatively limited [20, 21], especially comparative experimental studies. In recent years, Wang et al. [22] conducted experiments concerning the fire response of point-supported single glazing. Nam et al. [23] investigated the failure of double glazing under a radiation condition. Debuyser et al [24] heated a small specimen of laminated glazing without framing to breakage. It is established that the various types of glass have a significant influence on their fire performance, but the different experimental condition in previous studies hinder effective comparison between them. To the authors' knowledge, there is no open literature concerning single, insulated and laminated glazing investigated under identical conduction. Thus, there is a lack of practical guidance about the optimization of glazing systems for the prevention of glass fallout in fires. What is more, in current structural fire design, glass surfaces are normally assumed open, and the process of the breakage of glass façades is ignored. The disadvantages of these assumptions are particularly evident in newly constructed buildings, where glass façades may resist the fire much longer than old windows. Considering the increasing use of different kinds of glazing in buildings, especially high-rise buildings, it is hence increasingly important to investigate their thermal breakage behavior and the underlying heat transfer mechanism.

In the present work, a total of ten full-scale experiments were conducted to explore the breakage behavior of the three most typical types of glazing: single coated, insulated and

laminated glass. A pool fire was used as the heat source. Measurements were carried out for surface and air temperatures, incident heat flux (HF), time to the occurrence of the first crack, crack initiation and propagation. Numerical simulations were performed to investigate and compare the heat transfer mechanisms in these glasses.

2. Experimental setup

As shown in Fig. 1(a), the experimental setup primarily consisted of the fire source, framing glazing and instrumentation. A 500×500 mm^2 pool fire was employed to provide the radiation source. N-heptane with a 99% mass fraction was used as fuel and its mass and distance from the glass pane were adjusted depending on each experimental requirement. It should be noted that a pool fire cannot provide as uniform thermal loading as a radiation panel, but it may model a real fire situation especially the great thermal shock. In addition, its fire load and location can be easily changed to achieve the experimental purpose, as has been proved reasonable in previous work [22]. Fig. 1(b) shows that a well-designed frame made of stainless steel, which can withstand 1200 °C, was used to support the glass pane: in the thickness direction, the glass pane was clamped using several thin strips, and the clamping pressure could be controlled by revolving screws. The width of the covered region at the edge was 20 mm. This design ensured that different types of glazing could be well installed and restrained under almost identical conduction, which helps to satisfy the comparison purpose. In the aspect of inducing a thermal gradient, this framing design and real framing have a similar influence on the glazing pane, so the substantial characteristic is considered identical. Tests were conducted for: 1) single coated float glazing, 2) insulated glazing consisting of two clear float glass panes separated by a 6 mm thick air-filled space, and 3) laminated glazing

consisting of two clear float glass panes with a 0.38 mm interlayer of polyvinyl butyral (PVB) film. It should be noted that the dimensions of all the single panes were 600×600×6 mm^3 and all the glass panes were float glass, namely not tempered glass, and made of identical materials by the same local manufacturer. The cross-sections of the three different types of glazing are sketched in Fig. 1(c). All the glass panes were installed in the form of exposed framing glazing, and the condition of an actual glazing unit was approximated as closely as possible.

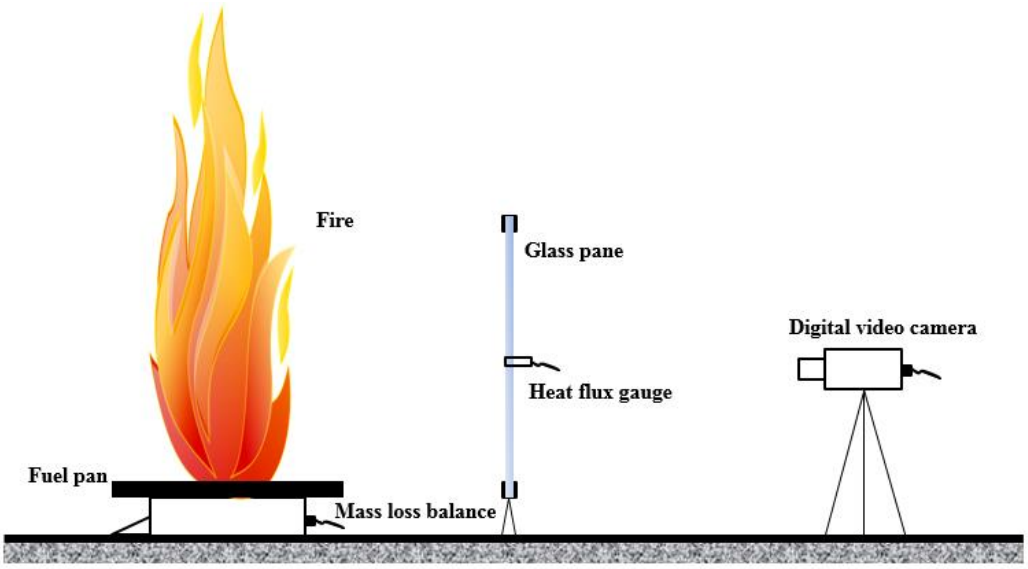

(a) The experimental system.

(b) The exposed framing glass.

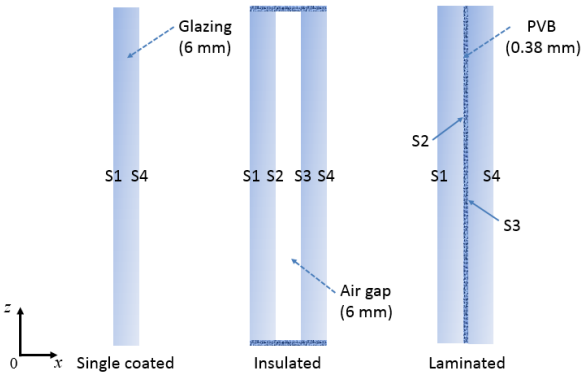

(c) The cross sections of three types of glazing.

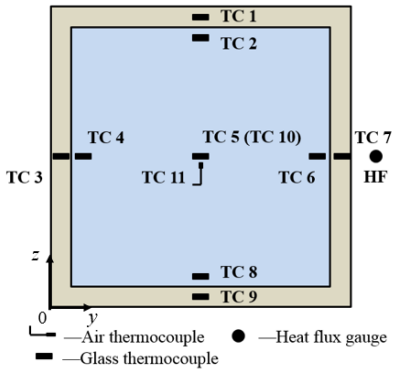

(d) The distribution of thermocouples and heat flux gauge.

Fig. 1. The schematic of the experimental system in the fire.

Sheet K-type thermocouples were attached to the glass panes using high-temperature resistant adhesive. For the insulated and laminated glass, the glass pane on the fire side is named Pane 1 and the other is Pane 2. The four surfaces are named S1, S2, S3 and S4 from the fire side to the ambient side. For comparison, the ambient surface of the single glazing is also named S4, as shown in Fig. 1(c). The thermocouples are numbered TC1-TC10: only TC10 was attached on the ambient side surface (S4), while the other nine thermocouples were on the fire side surface (S1). In addition, a sheathed thermocouple with a diameter of 1 mm, numbered TC 11, was positioned 5 mm in front of the glass to measure the air temperature. The thermocouples were made by a professional local manufacturer, with a measurement range of 0-1200 ºC and sensitivity of 41 μV/ºC. Due to the minor influence of a smoke layer or fire growth, the uncertainty of temperature measurement is evaluated at ±5% in the present work, which is much less than that in compartment fire experiments (uncertainty 10-30%) [13, 20]. A data acquisition system with 16 channels for the thermocouples was used, with the sampling time adjusted to 1 s. A Gardon water-cooled total heat flux gauge (MEDTHERM 64 series) with a measurement range of 0-50 kW/m^2 was employed to measure the incident heat flux on

the glass. The sensitivity of the gauge is 0.8750 mV/(kW/m^2). It can work well under 800 °C. The manufacturer's literature for Gardon type gauges indicates that the accuracy is ~±3%, but it will rise to ~±8-14% when used in a fire environment [25]. It is not possible to drill into the glass sections to mount the gauges. Mounting the gauges directly in front of the glass sections is not desirable either since the gauges would be shielding the glass sections from the radiation of the fire. Thus, the gauge was fixed off to the side of each glass pane and mounted flush to the surface of the glass sections so as to situate them as close to the measurement location as possible. This method has been used extensively to obtain heat flux data for glazed sections [14, 20]. The fire side of the glass pane was monitored by a standard video camera (SONY HDR-PJ790E) with a framing rate of 50. The distribution of all the thermocouples is shown in Fig. 1(d). To clearly depict the specific position of the glass pane, a coordinate system is created, setting the lower left corner as the origin point and the unit as mm.

A total of ten glass panes, including single coated, insulated and laminated glazing, were heated until breakage. To achieve the experimental purpose, the fuel mass was varied from 2 kg to 6 kg, and the distance between the glass pane and the burner center was adjusted from 750 mm to 450 mm. The overall cases are summarized in Table 1.

Table 1. The summary of experimental tests.

Test number	**Glass type**	**Burner-glazing distance (mm)**	**Mass of fuel (kg)**
1-4	Single coated	750	2
5	Insulated	750	2
6	Insulated	750	4
7-8	Insulated	450	6
9	Laminated	750	2

10	Laminated	750	4

3. Experimental results

3.1 Breakage time and fracture behavior

The first breakage times are listed in Table 2. All the single coated glazing and the fire side pane of the double glazing broke. For the coated glass, 2 kg fuel was used, providing a maximum heat release rate (HRR) of 300 kW. The breakage times in the four tests were found to be very similar with an average value of 157 s, which is significantly shorter than that of clear float glass (214 s) under an identical experimental condition [26]. This difference may be attributed to the surface flaws caused by the coating process during manufacturing, which can significantly reduce the practical strength of a glass product [27].

With regard to the insulated glazing, Pane 1 acted as a band pass filter, blocking the flames and hot gas layers beyond the first pane exposed in multi-pane glazing [10, 28]. Meanwhile, the air between the two glass panes could significantly reduce heat conduction in the double glazing unit. When the glass pane was positioned 750 mm from the fire, Pane 1 broke easily. The maximum temperature on S4 only reached 52 °C and 55 °C respectively in Tests 5 and 6, so no crack occurred in Pane 2. To achieve the breakage condition of Pane 2, the fuel mass was increased to 6 kg with the maximum HRR of 700 kW, and the burner-glazing distance was decreased to 450 mm. In Test 8, Pane 2 broke at 366 s, which was several times longer than for the single glazing. In Tests 9 and 10, the laminated glasses were tested. The fuel mass was increased in Test 10 to verify if any fallout would occur in laminated glazing after a greater thermal loading. Both panes in each test broke. Unlike insulated glazing, the laminated glass is separated

by a PVB film whose heat conductivity coefficient is ten times that of air. Thus, the maximum temperature on S4 was 110 °C, which was sufficient to result in the breakage of Pane 2.

The air gap and Pane 1 can provide good protection for Pane 2, so insulated glazing may remain intact for a relatively long period. Although the laminated glass was found to be more prone to breakage than insulated glass, the whole unit can still hold together after crack formation and propagation, preventing a new vent forming. It should be noted that when the fuel mass was increased, the time to the first crack actually increased as found in Tests 5-6 and Tests 9-10. This is caused by the combustion characteristic of pool fire: the thicker fuel needs more time to reach a high HRR after ignition [29].

Table 2. Breakage time and crack initiation location.

Test number	**Time of first crack occurrence (s)**		**The first crack position, coordinate (viewed from fire side)**	
1	143		Right edge, (600, 267)	
2	167		Left edge, (0, 354)	
3	147		Left edge, (0, 441)	
4	169		Right edge, (600, 368)	
	Pane 1	Pane 2	Pane 1	Pane 2
5	143	No breakage	Left edge, (0, 460)	No breakage
6	253	No breakage	Right edge, (600, 215)	No breakage
7	113	No breakage	Left edge, (0, 443)	No breakage
8	76	366	Left edge, (0, 388)	Right edge (600, 215)
9	118	199	Left edge (0, 379)	Left edge (0, 395)
10	258	332	Left edge (0, 381)	Left edge(0, 385)

In the present study, since the glass panes were four-edge covered, as shown in Table 2,

all the cracks initiated from the pane edges which contain many more imperfections caused by cutting and installing [30]. This phenomenon is consistent with previous window glazing tests [31, 32]. In addition, the width of the fire plume was slightly smaller than that of the glass pane, resulting in a relatively great thermal gradient along the horizontal direction. As a consequence, all the cracks were initiated on the left or right edges, particularly within 200-400 mm of the *z* coordinate. Because four edges were covered in Pane 1 and none were covered areas in Pane 2, the temperature gradient between the center and the edges of Pane 2 was much less than that with the frame coverage, which also contributed to the longer breakage time. For the insulated glazing, the crack initiations in the two panes were sometimes different. For the laminated glass, the location of crack initiation in Pane 2 was nearly the same as Pane 1 due to the close bonding.

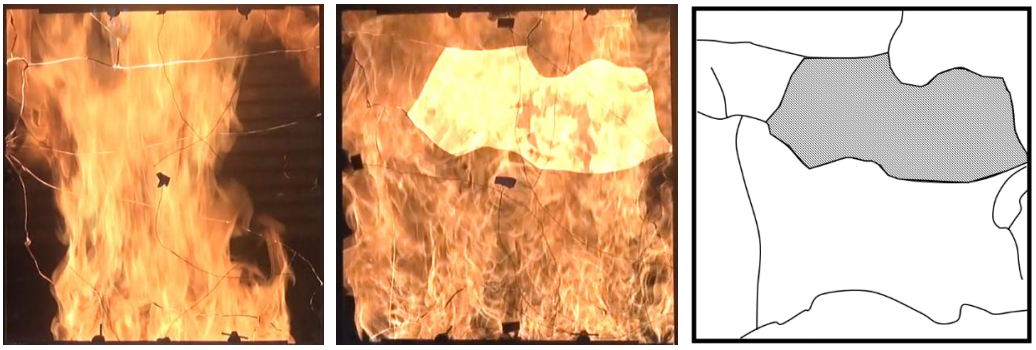

(a) Crack and fallout of single coated glass pane in Tests 1 and 2

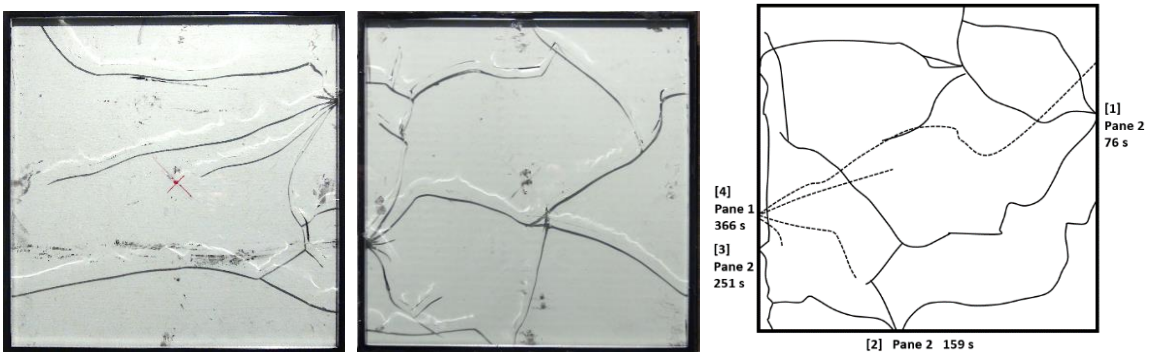

(b) Crack path of insulated glass in Tests 5, 6 and 8

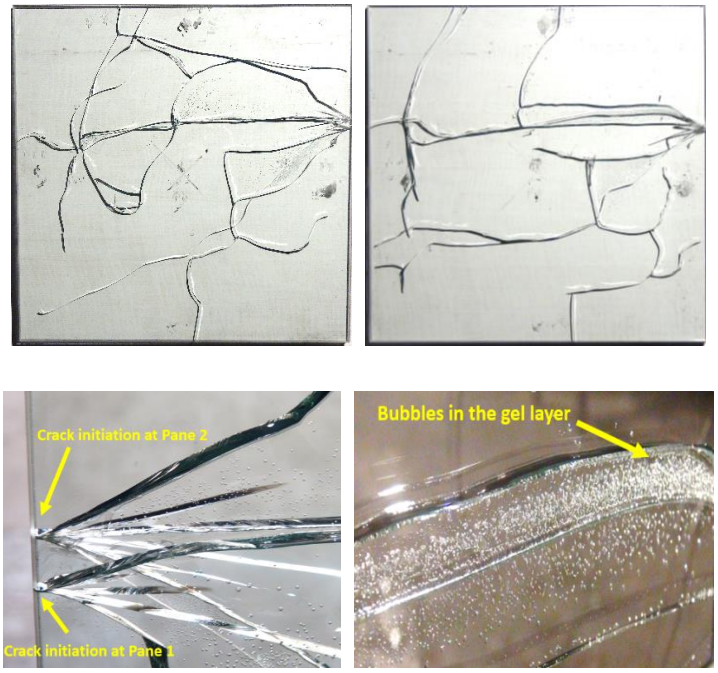

(c) Crack path of laminated glass in Tests 9 and 10

Fig. 2. The crack and fallout of glass (viewed from the ambient side).

Figure 2 shows the final post-crack path of the single coated, insulated and laminated glasses. After crack initiation, the crack propagated to the center of the glass pane, bifurcating and crossing. Then, islands formed, resulting in pieces of glass falling out. In a compartment fire, because of the influence of smoke movement and pressure variance, fallout is more likely to occur. However, among the ten tests conducted in an open space, fallout only occurred in Test 2 as shown in Fig. 2(a). The fallout occurred as soon as the first crack was initiated, with a proportion of 20%. It appears that single glazing is more prone to fallout than double-glazed units. However, for the laminated glass, gases such as water vapor, carbon dioxide and hydrogen chloride [33] were emitted from the interlayer when its temperature reached approximately 200 °C. Thus, a large number of bubbles appeared in the interlayer after heating, especially along the crack path where more heat may go through, as shown in Fig. 2(c). More bubbles appeared in Test 10 because of the

fuel mass increase. If the fire could last longer, it is believed that the interlayer and perimeter binder would be pyrolyzed and carbonized, considerably weakening the integrity of the glazing unit. What is more, toxic smoke from the interlayer may be released once overheated [34], which will aggravate the fire hazard. Therefore, improving the fire resistance of interlayers is critical for the prevention of crack and fallout and needs to be studied further in the future [5].

3.2 Temperature and heat flux

Surface temperature and incident heat flux are the most important parameters for the occurrence of glass breakage. As typical examples, the temperature variance of Tests 1, 6 and 9 are shown in Fig. 3. It can be seen that two types of temperature curves appear: the temperatures in the exposed area and the temperatures in the covered area. In addition, for most of the time, the air temperature was lower than the glass surface temperature in the center, indicating that the primary heat transfer mode from the fire was thermal radiation. Because the experiments were conducted in an open space, the HRR of the pool fire was stabilized. Assuming constant incident heat flux and neglecting convection, the glazing temperature may increase linearly according to the following equation [21]:

$$mc\frac{\mathrm{d}T_g}{\mathrm{d}t} = q(t)A - hA(T_g - T_\infty) \tag{1}$$

where m, c and A are respectively the mass, specific heat and surface area of the glass pane; h is the convection heat transfer coefficient; q is the incident heat flux; T_g and T_∞ are the glass temperature and ambient air temperature. This explains why the temperature in Tests 6 and 9 increased nearly linearly.

On the other hand, the glass surface temperature difference is of great importance to glass breakage. To investigate this issue, the temperature difference on the glass surface is

defined as:

$$\Delta T = \frac{(T_2 - T_1) + (T_4 - T_3) + (T_6 - T_7) + (T_8 - T_9)}{4} \quad (2)$$

where T_i is the temperature measured by TCi. In Test 1, the center temperature and temperature difference were respectively 89 °C and 54 °C at the time of the first crack occurrence. In Tests 6 and 9, the critical temperature differences of Pane 1 were 83 °C and 96 °C. All the critical values of Pane 1 are listed in Table 3, in which the temperature differences are calculated according to Eq. (2). It was found that for single coated glazing (Tests 1-4), the temperature differences at breakage time were distributed in the range of 54-68 °C, which is considerably lower than the 64-96 °C found for clear glass (Tests 5-10). These results further suggest that clear glass has better fire resistance than coated ones. In addition, at the time of the first breakage, the air temperatures were all lower than the corresponding temperatures at the center of the glass pane (TC5).

Tests 6 and 10 were conducted under identical experimental conditions: 4 kg fuel and 750 mm glazing-burner distance. Thus, their ambient surface temperatures were selected for comparison of the heat transfer as shown in Fig. 3(d). The results suggest that the insulated glazing has a much better thermal insulation than the laminated one. Among the ten tests, the breakage of Pane 2 only occurred in Tests 8-10. Although their breakage times were considerably different, the temperatures at the center of S4 are very similar, as listed in Table 4.

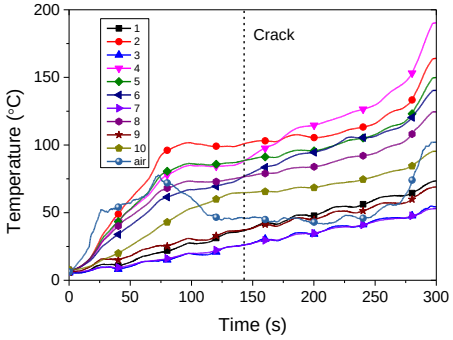

(a) Temperature variance in Test 1

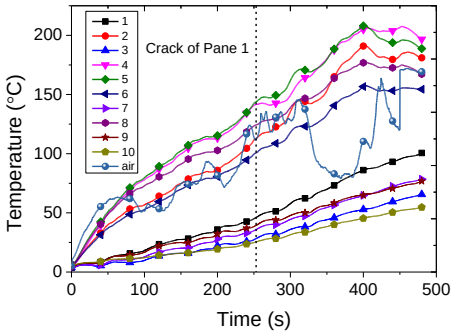

(b) Temperature variance in Test 6

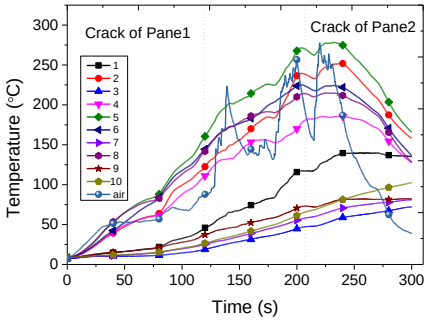

(c) Temperature variance in Test 9

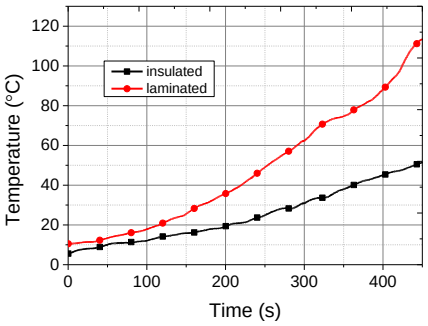

(d) Comparison of TC 10 between Tests 6 and 10

Fig. 3. The temperatures at different monitoring points.

Table 3. Important parameters at the time of Pane 1 breakage.

Test number	Central temperature, TC5 (°C)	Air temperature, TC11 (°C)	Temperature difference (°C)	Total heat flux (kW/m^2)
1	89	46	54	11.45
2	127	63	55	9.23
3	104	54	68	9.00
4	101	58	60	13.14
5	127	45	64	9.23
6	144	105	83	11.57
7	184	126	77	5.72
8	165	128	64	9.40

9	156	88	96	10.98
10	181	123	79	9.93

Table 4. Important parameters at the time of Pane 2 breakage.

Test number	**Central temperature on S4, TC10 (°C)**	**Total heat flux (kW/m^2)**
8	84	54.90
9	61	14.31
10	73	13.43

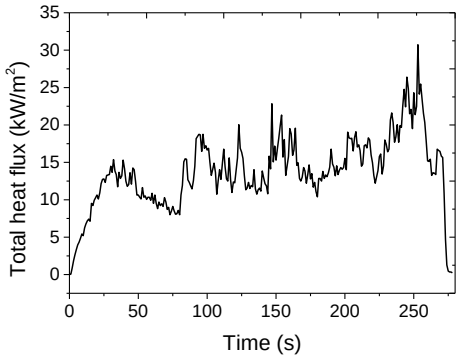

(a) HF of Test 5, 2 kg fuel

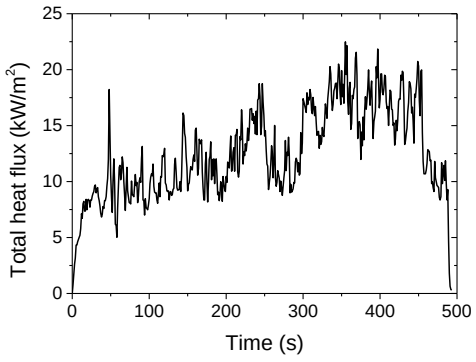

(b) HF of Test 10, 4 kg fuel

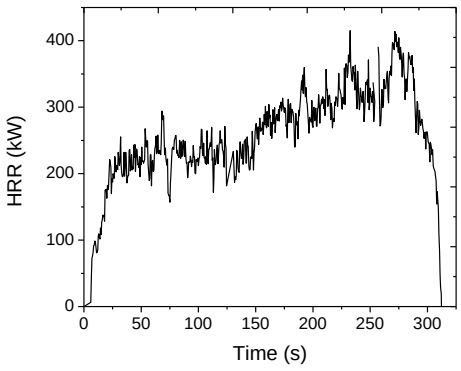

(c) HRR of Test 1, 2 kg fuel

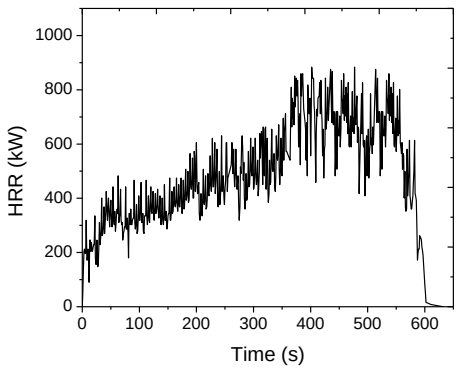

(d) HRR of Test 8, 6 kg fuel

Fig. 4. The total heat flux and heat release rate.

The variance of incident heat flux is the substantial cause of temperature increase. As

an example, the incident total heat fluxes in Tests 5 and 10 are shown in Fig. 4(a) and (b). Despite different burning times (278 s and 493 s), both curves are relatively steady at 10-25 kW/m^2 after ignition. Because the tests were carried out in an open space, the variation of the incident heat flux was similar to HRR. Fig. 4 (c) and (d) demonstrate the HRR of tests with 2 kg and 6 kg fuel mass, and it was found that the cracks were normally initiated in the steady stage. However, in enclosure fires, the incident thermal flux is directly proportional to time for the growing period of the fire [21]. As illustrated in Table 3, the critical heat flux was around 10 kW/m^2 for Pane 1, and its threshold value was 5.72 kW/m^2. This result is similar to the range of 4-5 kW/m^2 reported in a previous study [35]. Meanwhile, for Pane 2, the critical heat flux, with a threshold value of 13.43 kW/m^2, was found to be significantly larger than for Pane 1 or single glazing.

4. Discussion and comparison

4.1 Numerical model and its verification

Heat transfer is considered the primary cause of the varying thermal performance, especially for insulated and laminated glass. The commercial COMSOL Multiphysics finite element method (FEM) software was employed to predict the temperature on the glass surfaces [36]. From the experimental results, it is found that the temperatures measured in exposed (or covered) areas are very similar, confirming that in most areas of the glass surface relatively uniform thermal loading is imposed, so the thermal load is simplified as their average temperature. The thermal loading was extracted from Test 9 as shown in Fig. 5(a). The exposed temperature was the average of TC2, 4, 5, 6 and 8, while the covered temperature was the average of TC1, 3, 7 and 9. Uniform thermal loading was applied on the exposed and covered areas on S1. Following grid independence tests, a coarse grid was selected due to its computational efficiency and relatively good

accuracy. There were 29,441 tetrahedral elements, 14,264 triangular elements, 972 edge elements and 24 vertex elements in the 3D thermal analysis, as shown in Fig. 5(b). The time interval was set at 1 sec. The physical properties of the glass, PVB and air, obtained from previous work [10, 37], are listed in Table 5. Numerical simulations were performed to simulate the temperature variance of the glazing. In the numerical simulation, the glass is generally heated and conducts heat in the *x*, *y* and *z* directions:

$$\rho c \frac{\partial T}{\partial t} + \nabla \cdot q = Q \tag{3}$$

$$q = -k\nabla T \tag{4}$$

where ρ, c and k are the density, specific heat and thermal conductivity of the glazing; Q represents the heat source. The specific heat transfer progress can be explained as follows: on S1, the glass receives radiation from the fire. Meanwhile, it radiates to the ambient, convects with air and conducts heat into the glass pane:

$$-n \cdot k\nabla T = h \cdot \left(T_\infty - T\right) + q - \varepsilon\sigma T^4 \tag{5}$$

where ε is the emissivity of the glass surface; σ is the Stefan-Boltzmann constant; n is the direction vector. On S4, heat is released to the ambient by convection and radiation:

$$-n \cdot k\nabla T = h \cdot \left(T_\infty - T\right) + \varepsilon\sigma(T_{\text{sur}}^4 - T^4) \tag{6}$$

where T_∞ and T_{sur} are 280.15 K according to the experimental condition. The convection heat transfer coefficient *h* is 40 W/(m^2·K) [17]. The sketch of this heat transfer model is shown in Fig. 5(c).

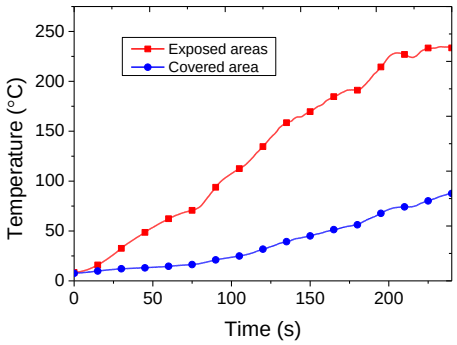

(a) Thermal loading extracted from Test 9

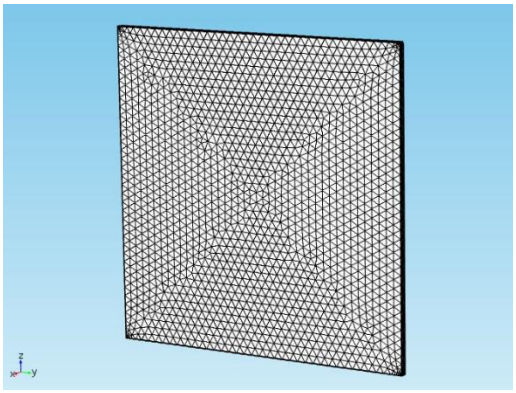

(b) Mesh grid of laminated glass

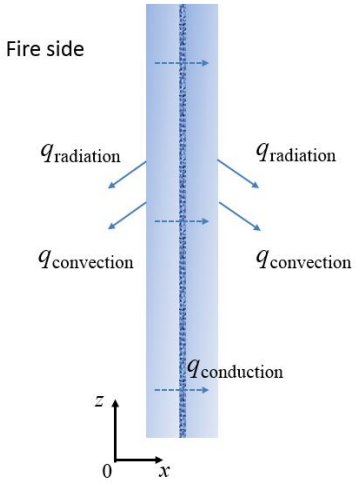

(c) Sketch of the heat transfer model for laminated glazing.

Fig. 5. Thermal loading and mesh generation in the simulation.

Table 5. The properties of glass, PVB and air employed in simulation [10, 37].

Properties	**Symbol**	**Value**
	Glass	
Density (kg/m^3)	ρ	2500
Modulus of elasticity (Pa)	E	7.3×10^{10}
Poisson's ratio	ν	0.17
Thermal expansion coefficient (1/K)	β	8.46×10^{-6}
Reference temperature (K)	T_R	280
Specific heat capacity (J/(kg·K))	c	820
Thermal conductivity (W/(m·K))	k	0.94

Emissivity	ε	0.85
	PVB	
Density (kg/m^3)	ρ_{PVB}	1070
Specific heat capacity (J/(kg·K))	c_{PVB}	1100
Thermal conductivity (W/(m·K))	k_{PVB}	0.221
	Air (300 K)	
Density (kg/m^3)	ρ_{air}	1.16
Specific heat capacity (J/(kg·K))	c_{air}	1007
Thermal conductivity (W/(m·K))	k_{air}	0.0263

Then, the temperature distribution of Test 9 was calculated. To verify the simulation, the temperature measured by TC10 in Test 9 and the numerical result are compared in Fig. 6(a). It is found that their maximum difference is less than 5 °C. The good agreement between the experimental and numerical results indicates the reliability of the model. The model was hence used to calculate the central temperatures of S1-S4 and plotted in Fig. 6(b). Since the temperature on S2 and S3 cannot be measured in the experiments, the calculated values are helpful for revealing the heat transfer mechanism in laminated glass. It can be seen that the temperature decreases by about 50% in both Pane 1 and Pane 2. Because the primary heat transfer in the laminated glass was by means of conduction, the temperature increase on S2 and S3 lagged considerably behind S1. When the fire went out at 274 s, the temperature of S4 was still increasing fast. In addition, to determine the critical breakage condition of Pane 2, the temperatures at the center and edge are shown in Fig. 6(c). It is established that the frame protection has a significant influence on the S3 temperature, inducing a large thermal gradient in Pane 2. The temperature difference at breakage time is 66 °C, which is similar to the critical condition of Pane 1. The S3

temperature distribution at breakage time is shown in Fig. 6(c) for confirmation.

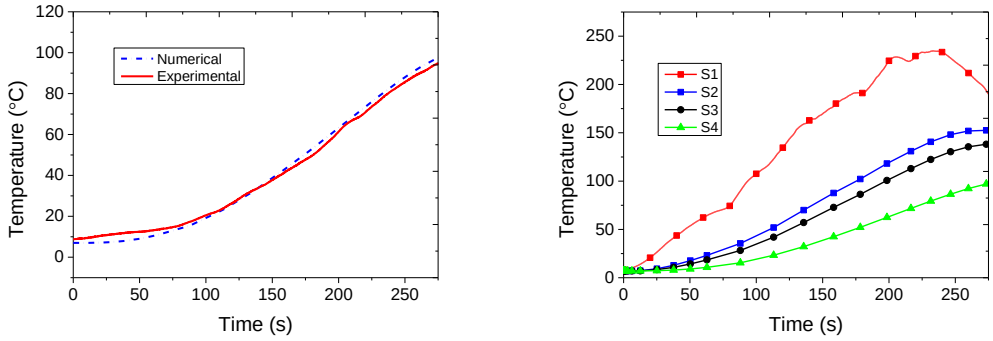

(a) Experimental and numerical comparison of S4 temperature (b) Temperatures on four surfaces

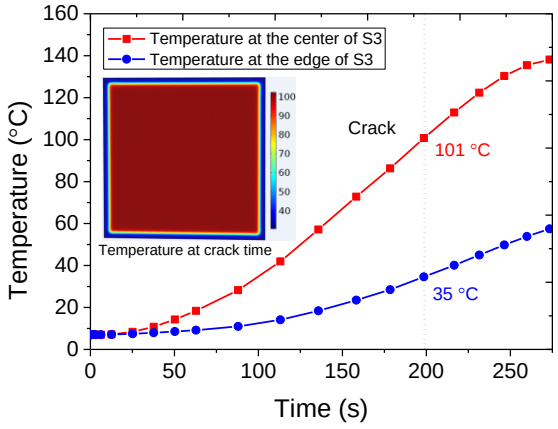

(c) The temperature variance on S3

Fig. 6. The calculated temperatures of Test 9.

4.2 Comparison of different glazing types

To compare the heat transfer mechanism in the three different glasses, the thermal resistance of glazing is expressed here. For single glazing, the thermal resistance caused by the convection on S1, the conduction in glazing, and convection on S4 is:

$$R_{single} = \frac{1}{h_{S1}A} + \frac{\delta}{k_g A} + \frac{1}{h_{S4}A} \tag{7}$$

where R is the thermal resistance; δ is the glass thickness; h_{s1} and h_{s4} are the convection heat transfer coefficients on S1 and S4; k_g is the thermal conductivity of glass. For the

insulated glazing studied in the work, the air gap thickness is 6 mm, less than the critical thickness of 10 mm, so the conduction through the stagnant air is the dominant transport mechanism [28]. Assuming that the air between glass panes is stagnant, then the heat resistance is:

$$R_{\text{insulated}} = \frac{1}{h_{S1}A} + \frac{\delta}{k_g A} + \frac{1}{h_{S2}A} + \frac{L_{air}}{k_{air}A} + \frac{1}{h_{S3}A} + \frac{\delta}{k_g A} + \frac{1}{h_{S4}A} \tag{8}$$

where δ is the glass thickness; L is the thickness of the air gap; k_{air} is the thermal conductivity of the air gap. For laminated glass, although there is no heat convection between the glazing and PVB, the contact resistance cannot be ignored, which is due principally to the surface roughness effect [37]. Thus, the thermal resistance of laminated glass is:

$$R_{\text{laminated}} = \frac{1}{h_{S1}A} + \frac{\delta}{k_g A} + R_{\text{c}} + \frac{L_{\text{gel}}}{k_{\text{gel}}A} + R_{\text{c}} + \frac{\delta}{k_g A} + \frac{1}{h_{S4}A} \tag{9}$$

where R_c is the thermal contact resistance.

If the radiation heat transfer between the glazing and ambient is small and ignored [17, 21], the above equations clearly demonstrate that the single glazing has the less thermal resistance among the three glazing categories. As the surface of glazing is smooth, its contact resistance is normally small, thus it does not contribute much to the thermal resistance of laminated glass. Owing to the thicker gap (6>0.38 mm) and lower heat conductivity coefficient (air 0.0263<PVB 0.221 W/(m·K)), insulated glazing has the greatest thermal resistance.

In addition, the S4 temperatures of single, insulated and laminated glass are compared. The boundary condition and grid resolutions are the same as the above simulation. For insulated glazing, the air gap is assumed to be stagnant and its pressure rise caused by

heating is neglected; conduction rather than convection through the stagnant air dominates the transport mechanism [28]. The comparison of the S4 temperature variance is illustrated in Fig. 7(a). The order of the temperature increase rate on S4 is single>laminated>insulated, and the difference is significant. In addition, the *x*-*z* cross-sections in the middle of the glass pane at 250 sec are plotted in Fig. 7(b). The heat conduction in the *x* direction determines the breakage occurrence of the glazing. In the *z* direction, the heat transfer in single glazing is also much more significant than the other two glasses. The numerical result confirms the theoretical analysis, which suggests that the insulated glazing has the greatest fire resistance. For insulated glazing, the radiation between the two glass panes is highly dependent on the emissivities of the two interior surfaces. A simulation considering inter-pane radiation is conducted and shows a slightly higher temperature on S4 (less than 3 ºC) at an early stage than the curve in Fig. 7(a). It should be noted that the potential risk of fallout in Pane 1 may be the primary cause of the rapid temperature increase of Pane 2 [28].

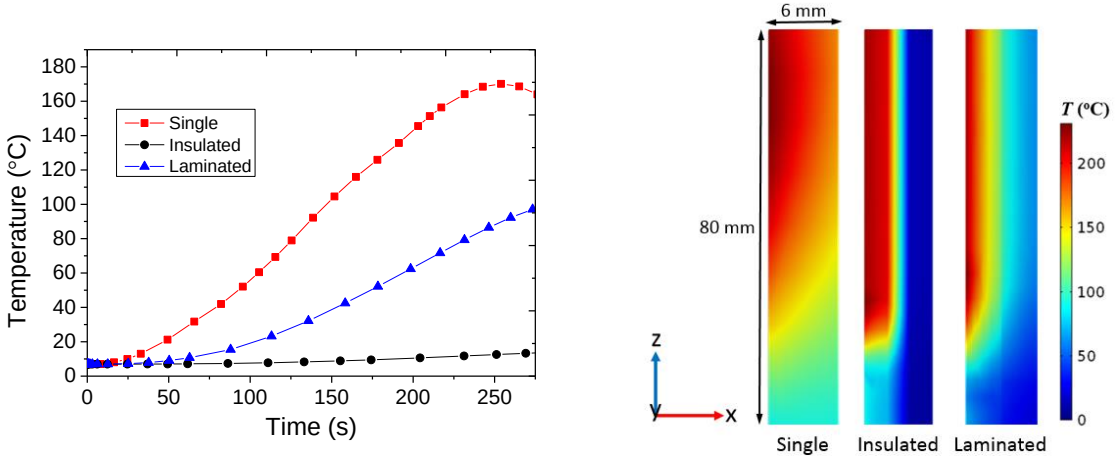

(a) S4 temperatures (b) Temperature distribution in thickness at 250 s

Fig. 7. The temperature comparison of three different types of glazing.

4.3 Application suggestion

Joshi and Pagni [18] have developed a simplified mathematical model, BREAK1, which can be used to estimate the time for a window to break when exposed to a compartment fire. From the experimental results, the heat flux is assumed to increase to around 11 kW/m^2 at 30 s and then remain constant. The hot air temperature is set as 50 ºC. The other parameters are extracted from Table 5. The calculated breakage time is 135 s, which is conservative compared with the experimental results. The prediction shows that the glass will break when the central temperature is 97 ºC, which falls in the temperature range of 89-127 ºC recorded in our tests. In the work of Manzello et al. [20], a glass wall assembly was exposed to an intense real-scale compartment fire with a maximum incident heat flux of about 170 kW/m^2. The results show that all the single glazing and the inside pane of the laminated glazing broke and fell out during the fire, but the outside glass pane for double-pane glass sections remained intact throughout the fire exposure and did not crack. Shields et al. heated non-tempered single and insulated glazing in ISO room using pool fires with different sizes [14, 21]. When a 0.9×0.9 m^2 pool fire with a maximum heat flux of 80 kW/m^2 was employed, the average breakage time of single glazing was around 1 min [14], while for the outer pane of insulated glazing it was more than 4 min [21]. However, the fallout of the outer pane with a maximum proportion of 85% occurred when the pool fire was larger than 0.8×0.8 m^2.

The limited literature concerning these three types of glazing investigated under similar conduction hinders an effective comparison between them. In the present work, Tests 1-5 and 9, including three types of glazing, were performed under identical conditions. The experimental results can be used directly in the fire resistance evaluation of different glasses. Both an application suggestion and the critical breakage condition are obtained. Based on the previous and present work, it is confirmed that the double-glazed

unit has markedly better thermal resistance than single glazing, and can thus survive 4-5 times longer in a fire. However, between the two typical double-glazed units studied in this work, it is necessary to dialectically determine which is better when subjected to a fire. The breakage of Pane 2 represents the failure of the double-glazed unit. The temperature of Pane 2 in the laminated glass may increase faster than insulated glazing, causing it to reach the critical temperature difference more quickly. This occurred in both Tests 8-10 and the numerical simulations. Nevertheless, only the fallout of glass can change the fire dynamics in a compartment, thus from this aspect, the laminated glass may be a more reasonable choice since it can remain intact even after both panes break.

It should be noted that more repeated tests in realistic framing systems need to be conducted in a real compartment fire, which may include the effect of moving smoke and pressure variance. It is anticipated that fallout would occur more easily than in the present work [28]. In addition, only the thermal field is predicted above, whereas a more advanced numerical model considering the stress distribution and fallout of Pane 1 would help provide a more accurate prediction. In addition, all the above suggestions are provided only based on their fire performance, and other factors also need to be considered in building construction. For example, single glazing can reduce the weight of a building façade, and it is much less expensive than insulated and laminated glasses. To give a clear comparison, the strengths and weaknesses of the three different types of glazing are summarized in Table 6.

Table 6. The summary of strength and weakness of different glasses.

Glass type	**Strength**	**Weakness**
Single glazing	Lighter, lower expense	Falling out the most easily
Insulated glazing	Insulation	Falling out easily

Laminated glass	Good integrity	Most expensive

5. Conclusions

A total of ten tests were conducted to study the fire performance of three different typical glasses. Breakage time, glass surface and air temperature, incident heat flux and crack initiation and propagation were obtained. Numerical simulations were also carried out to gain an insight on the heat transfer in single and double glazing systems. The following conclusions may be drawn:

1) The single glazing and Pane 1 in the double-glazed unit have similar critical breakage conditions: a temperature difference of 60-90 °C, and total heat flux of around 6 kW/m^2. The breakage of Pane 2 requires significantly higher heat flux (more than 13 kW/m^2), but its breakage also occurred at a temperature difference of approximately 60 °C.

2) All the cracks were initiated from the glass pane edge, but the fallout occurs most easily in single glazing. Owing to the PVB bonding, laminated glass can remain intact after the failure of the whole glazing unit, demonstrating its capability to prevent new vents forming in enclosure fires.

3) The heat transfer mechanism of the three different glasses was investigated by FEM analysis. The insulated glazing demonstrates the best insulation and protection for Pane 2 assuming no fallout in Pane 1. However, the heat transfer mechanism of insulated glazing still needs to be further investigated.

4) The selection of the glass category should be evaluated in many aspects. From the standpoint of fire safety, laminated glass is highly recommended in high-rise building construction. Its capability to prevent glass fallout and the creation of fire vents can

effectively prevent fire spreading rapidly to different floors of a building.

Acknowledgments

This work is supported by National Natural Science Foundation of China (Grant no. 51578524), Youth Innovation Promotion Association CAS (Grant no. 2013286) and Research Grants Council of the Hong Kong Special Administrative Region, China (Project No. 9042221, CityU 11300215).

References

[1] I. Pérez-Grande, J. Meseguer, G. Alonso, Influence of glass properties on the performance of double-glazed facades, Appl. Therm. Eng., 25(17) (2005) 3163-3175.

[2] M. Bojić, F. Yik, Application of advanced glazing to high-rise residential buildings in Hong Kong, Build Environ, 42(2) (2007) 820-828.

[3] C. Zhang, J. Wang, X. Xu, F. Zou, J. Yu, Modeling and thermal performance evaluation of a switchable triple glazing exhaust air window, Appl. Therm. Eng., 92 (2016) 8-17.

[4] Y. Wang, Q. Wang, J. Sun, L. He, K.M. Liew, Influence of fire location on the thermal performance of glass façades, Appl. Therm. Eng., 106 (2016) 438-442.

[5] M. Quinn, A. Nadjai, F. Ali, A. Abu-Tair, Experimental and Numerical Investigation of Localised Fire on Glazing Facades Having Different Orientations, Journal of Structural Fire Engineering, 4(3) (2013) 153-164.

[6] G. Gan, Thermal transmittance of multiple glazing: computational fluid dynamics prediction, Appl. Therm. Eng., 21(15) (2001) 1583-1592.

[7] L.H. Lin, E. Hinman, H.F. Stone, A.M. Roberts, Survey of window retrofit solutions for blast mitigation, Journal of performance of constructed facilities, 18(2) (2004) 86-94.

[8] Q. Wang, Y. Wang, Y. Zhang, H. Chen, J. Sun, L. He, A stochastic analysis of glass crack initiation under thermal loading, Appl. Therm. Eng., 67(1–2) (2014) 447-457.

[9] H. Emmons, The needed fire science, in: Fire Safety Science-Proceedings of the First International Symposium, IAFSS, 1986, pp. 33-53.

[10] P. Pagni, Thermal glass breakage, in: Fire Safety Science-Proceedings of the Seventh International Symposium, IAFSS, Worcester, Massachusetts, USA, 2002, pp. 3-22.

[11] O. Keski‐Rahkonen, Breaking of window glass close to fire, II: circular panes, Fire Mater., 15(1) (1991) 11-16.

[12] O. Keski‐Rahkonen, Breaking of window glass close to fire, Fire Mater., 12(2) (1988) 61-69.

[13] T.J. Shields, G.W.H. Silcock, M. Flood, Performance of a single glazing assembly exposed to a fire in the centre of an enclosure, Fire Mater., 26(2) (2002) 51-75.

[14] T.J. Shields, G.W.H. Silcock, M.F. Flood, Performance of a single glazing assembly exposed to enclosure corner fires of increasing severity, Fire Mater., 25(4) (2001) 123-152.

[15] A. Joshi, P. Pagni, Fire-induced thermal fields in window glass. II—experiments, Fire Saf. J., 22(1) (1994) 45-65.

[16] A.A. Joshi, P.J. Pagni, Fire-Induced Thermal Fields in Window Glass .1. Theory, Fire Saf. J., 22(1) (1994) 25-43.

[17] K. Harada, A. Enomoto, K. Uede, T. Wakamatsu, An experimental study on glass cracking and fallout by radiant heat exposure, in: Fire Safety Science—Proceedings of the Sixth International Symposium, IAFSS, 2000, pp. 1063-1074.

[18] A.A. Joshi, P.J. Pagni, Users' guide to BREAK1, the Berkeley algorithm for breaking window glass in a compartment fire, National Institute of Standards and Technology, Building and Fire Research Laboratory, 1991.

[19] Q. Wang, H. Chen, Y. Wang, J.X. Wen, S. Dembele, J. Sun, L. He, Development of a dynamic model for crack propagation in glazing system under thermal loading, Fire Saf. J., 63(0) (2014) 113-124.

[20] S.L. Manzello, R.G. Gann, S.R. Kukuck, K.R. Prasad, W.W. Jones, An experimental determination of a real fire performance of a non-load bearing glass wall assembly, Fire Technol., 43(1) (2007) 77-89.

[21] J. Shields, G.W. Silcock, F. Flood, Behaviour of double glazing in corner fires, Fire Technol., 41(1) (2005) 37-65.

[22] Y. Wang, Q. Wang, G. Shao, H. Chen, Y. Su, J. Sun, L. He, K.M. Liew, Fracture behavior of a four-point fixed glass curtain wall under fire conditions, Fire Saf. J., 67(0) (2014) 24-34.

[23] J. Nam, H.-S. Ryou, D.-J. Kim, S.-W. Kim, J.-S. Nam, S. Cho, Experimental and Numerical Studies on the Failure of Curtain Wall Double Glazed for Radiation Effect, Fire Science and Engineering, 29(6) (2015) 40-44.

[24] M. Debuyser, J. Sjöström, D. Lange, D. Honfi, D. Sonck, J. Belis, Behaviour of monolithic and laminated glass exposed to radiant heating, Construction and Building Materials, 130 (2017) 212-229.

[25] T.K. Blanchat, C.R. Hanks, Comparison of the high temperature heat flux sensor to traditional heat flux gages under high heat flux conditions, Sandia National Laboratories (SNL-NM), Albuquerque, NM (United States), 2013.

[26] Y. Wang, Q. Wang, J. Sun, L. He, K. Liew, Thermal performance of exposed framing glass façades in fire, Mater. Struct., 49(7) (2016) 2961-2970.

[27] L. Wondraczek, J.C. Mauro, J. Eckert, U. Kühn, J. Horbach, J. Deubener, T. Rouxel, Towards ultrastrong glasses, Adv. Mater., 23(39) (2011) 4578-4586.

[28] B.R. Cuzzillo, P.J. Pagni, Thermal breakage of double-pane glazing by fire, J. Fire. Prot. Eng., 9(1) (1998) 1-11.

[29] B. Xu, Y. Zhang, J. Fang, S. Ma, Y. Liu, Study of heat release rate of normal heptane, Fire Science and Technology, 3 (2006) 304-307.

[30] S. Dembele, R.A.F. Rosario, J.X. Wen, Thermal breakage of window glass in room fires conditions – Analysis of some important parameters, Build Environ, 54(0) (2012) 61-70.

[31] Y. He, L. Poon, Experimental Observations And Modelling Of Window Glass Breakage In Building Fires, Fire Safety Science, 3 (1988) 295-306.

[32] M.J. Skelly, R.J. Roby, C.L. Beyler, An experimental investigation of glass breakage in compartment fires, J. Fire. Prot. Eng., 3(1) (1991) 25-34.

[33] M. Wu, W. Chow, X. Ni, Characterization and thermal degradation of protective layers in high‐rating fire‐resistant glass, Fire Mater., 39(1) (2015) 26-40.

[34] M. Wu, W. Chow, A review on fire-resistant glass with high rating, Journal of applied fire science, 23(1) (2013) 59-76.

[35] F.W. Mowrer, Window breakage induced by exterior fire, NIST-GCR-98-751, National Institute of Standards and Technology, Gaithersburg, MD, 1998.

[36] A. Comsol, COMSOL multiphysics user's guide, Version: September, 10 (2005) 333.

[37] T.L. Bergman, F.P. Incropera, D.P. DeWitt, A.S. Lavine, Fundamentals of heat and mass transfer, John Wiley & Sons, 2011.

Table captions

Table 1. The summary of experimental tests.

Table 2. Breakage time and crack initiation location.

Table 3. Important parameters at the time of Pane 1 breakage.

Table 4. Important parameters at the time of Pane 2 breakage.

Table 5. The properties of glass, PVB and air employed in simulation [10, 33].

Table 6. The summary of strength and weakness of different glasses.

Figure captions

Fig. 1. The schematic of the experimental system in the fire. (a) The experimental system; (b) The exposed framing glass; (c) The cross sections of three types of glazing; (d) The distribution of thermocouples and heat flux gauge.

Fig. 2. The crack and fallout of glass (viewed from the ambient side). (a) Crack and fallout of single coated glass pane in Tests 1 and 2; (b) Crack path of insulated glass in Tests 5, 6 and 8; (c) Crack path of laminated glass in Tests 9 and 10.

Fig. 3. The temperatures at different monitoring points. (a) Temperature variance in Test 1; (b) Temperature variance in Test 6; (c) Temperature variance in Test 9; (d) Comparison of TC 10 between Tests 6 and 10.

Fig. 4. The total heat flux and heat release rate. (a) HF of Test 5, 2 kg fuel (b) HF of Test 10, 4 kg fuel; (c) HRR of Test 1, 2 kg fuel (d) HRR of Test 8, 6 kg fuel.

Fig. 5. Thermal loading and mesh generation in the simulation. (a) Thermal loading extracted from Test 9; (b) Mesh grid of laminated glass; (c) Sketch of the heat transfer model for laminated glazing.

Fig. 6. The calculated temperatures of Test 9. (a) Experimental and numerical comparison of S4 temperature; (b) Temperatures on four surfaces; (c) The temperature variance on S3.

Fig. 7. The temperature comparison of three different types of glazing. (a) S4 temperatures; (b) Temperature distribution in thickness at 250 s.